

# Clumped stellar winds in supergiant high-mass X-ray binaries: X-ray variability and photoionization

L. M. Oskinova<sup>1, \*</sup>, A. Feldmeier<sup>1</sup>, P. Kretschmar<sup>2</sup>

<sup>1</sup> *Institute for Physics and Astronomy, University of Potsdam, 14476 Potsdam, Germany*

<sup>2</sup> *European Space Astronomy Centre (ESA/ESAC), Science Operations Department, Villanueva de la Caada (Madrid), Spain*

Accepted . Received ; in original form 21.02.2011 22:32

## ABSTRACT

The clumping of massive star winds is an established paradigm confirmed by multiple lines of evidence and supported by stellar wind theory. The purpose of this paper is to bridge the gap between detailed models of inhomogeneous stellar winds in single stars and the phenomenological description of donor winds in supergiant high-mass X-ray binaries (HMXBs). We use results from time-dependent hydrodynamical models of the instability in the line-driven wind of a massive supergiant star to derive the time-dependent accretion rate onto a compact object in the Bondi-Hoyle-Lyttleton approximation. The strong density and velocity fluctuations in the wind result in strong variability of the synthetic X-ray light curves. The model predicts a large scale X-ray variability, up to eight orders of magnitude, on relatively short timescales. The apparent lack of evidence for such strong variability in the observed HMXBs indicates that the details of accretion process act to reduce the variability due to the stellar wind velocity and density jumps.

We study the absorption of X-rays in the clumped stellar wind by means of a 2-D stochastic wind model. The monochromatic absorption in cool stellar wind in dependence on orbital phase is computed for realistic stellar wind opacity. We find that absorption of X-rays changes strongly at different orbital phases. The degree of the variability due to the absorption in the wind depends on the shape of the wind clumps and is stronger in case of oblate clumps.

We address the photoionization in the clumped wind, and show that the degree of ionization is affected by the wind clumping. A correction factor for the photoionization parameter is derived. It is shown that the photoionization parameter is reduced by a factor  $\mathcal{X}$  compared to the smooth wind models with the same mass-loss rate, where  $\mathcal{X}$  is the wind inhomogeneity parameter. We conclude that wind clumping must also be taken into account when comparing the observed and model spectra of the photoionized stellar wind.

**Key words:** accretion, X-rays: binaries, instabilities, stars: neutron, X-rays: stars

## 1 INTRODUCTION

Massive luminous OB-type stars possess strong stellar winds. The winds are fast, with typical velocities up to  $2500 \text{ km s}^{-1}$ , and dense, with mass-loss rates  $\dot{M} \gtrsim 10^{-7} M_{\odot} \text{ yr}^{-1}$ . The driving mechanism for the mass-loss from OB stars has been identified with radiation pressure on spectral lines (Castor et al. 1975, CAK). Early on Lucy & Solomon (1970) suggested that the stationary solution for a line-driven wind is unstable leading to shocks in stellar winds. Lucy & White (1980) proposed that the winds break up into a population of dense blobs. Owocki et al. (1988) performed numerical simulations of the nonlinear evolution of wind instabilities and showed that even small-amplitude perturbations in the radial velocity near the wind base result in a highly structured wind, with relatively slow, dense shells separated from regions of high-speed,

rarefied flow by strong shocks. Feldmeier et al. (1997a,b) used hydrodynamic simulations to model the evolution of wind instabilities and predicted the X-ray emission from single stars matching the observed X-ray fluxes. These non-stationary hydrodynamic simulations are used in this paper. Runacres & Owocki (2002) studied the evolution of wind structures and demonstrated that the winds can remain inhomogeneous out to distances of  $1000 R^*$ , while Dessart & Owocki (2005) presented first attempts of 2-D radiative hydrodynamic models of stellar winds.

These theoretical predictions of stellar wind clumping are confirmed by observations. From analysis of wind lines in the UV spectra Lucy (1982) postulated the existence of non-monotonic velocity fields in the winds. Hillier (1991) induced the existence of wind clumping from the shape of electron-scattering wings in emission lines of Wolf-Rayet (WR) stars. Stochastic variable structures in the He II  $\lambda 4686 \text{ \AA}$  emission line in an O-supergiant were found by Eversberg et al. (1998), and explained as excess emission from

\* E-mail: lida@astro.physik.uni-potsdam.de

the wind clumps. Markova et al. (2005) investigated the line-profile variability of  $H\alpha$  for a large sample of O-type supergiants. They concluded that the observed variability can be explained by a wind model consisting of coherent or broken shells. Lépine & Moffat (1999, 2008) presented direct spectroscopic evidence of clumping in O and WR star winds. Prinja & Massa (2010) established spectroscopic signatures of the wide-spread existence of wind clumping in B supergiants.

The inhomogeneity affects stellar wind diagnostics. Stewart & Fabian (1981) used *Einstein* spectra of O-stars to study the transfer of X-rays through a uniform stellar wind. By matching the model and the observed X-ray spectrum of the O-type supergiant  $\zeta$  Pup they found that the mass-loss rate derived from X-ray spectra is lower by factor of a few than the mass-loss rates obtained from fitting the  $H\alpha$  line as well as from observations at radio and IR wavelengths. As most plausible explanation for this discrepancy they suggested the neglect of the clumping in O-star winds. Waldron & Cassinelli (2001) proposed that a clumpy wind structure may help to explain the observed X-ray emission line profiles in the spectra of O-supergiants. A theory of X-ray transfer in clumped winds that accounts for clumps of any shapes and optical depths was first developed by Feldmeier et al. (2003); Oskinova et al. (2004). Indeed, accounting for wind clumping allows to consistently model the UV/optical and the X-ray spectra of O-stars (Oskinova et al. 2006).

Presently, clumping in first approximation (“microclumping”) is taken into account in all up-to-date stellar wind codes. This approximation assumes that clumps are optically thin and that the interclump medium is void. Microclumping leads to smaller empirical mass-loss rates when using diagnostics that depend on processes scaling with density squared ( $\rho^2$ ), such as  $H\alpha$  and other emission lines, or radio free-free emission (Hillier 1991; Hamann & Koesterke 1998). Bouret et al. (2005) and Fullerton et al. (2006) demonstrated that mass-loss rates must be reduced by orders of magnitude in order to reproduce the UV-resonant lines (which depend on density linearly) simultaneously with the  $\rho^2$  based diagnostics<sup>1</sup>. These drastic reductions of empirically deduced mass-loss rates would have strong consequences for the stellar evolution and stellar feedback models.

A way to solve this problem was suggested by Oskinova et al. (2007). It was found that waiving the microclumping approximation i.e. allowing for clumps of arbitrary optical depth (“macroclumping”) in the spectral models eliminates the need to strongly reduce stellar mass-loss rates. It was shown that the strength of optically thick diagnostic lines, such as the P V resonance line in OB star spectra, is reduced by macroclumping effects, while the strength of optically thin lines, such as  $H\alpha$ , is not affected. Therefore, accounting for macroclumping in analyzing stellar spectra yields empirically derived mass-loss rates that are only a factor 2–3 lower than the “classical” CAK mass-loss rates. These conclusions are confirmed by 2D model studies (Sundqvist et al. 2010) and full 3D radiative-transfer models (Šurlan et al., submitted).

The CAK mass-loss rates of massive stars are in good agreement with observed X-ray fluxes from high-mass X-ray binaries (HMXBs). HMXBs are the products of binary star evolution (e.g. Shklovsky 1967; Iben et al. 1995). These systems consist of an early-type massive star and a compact companion, neutron star (NS) or black hole (BH), on a close orbit. Accretion of stellar wind

**Table 1.** Stellar model parameters (see the full set of parameters in Feldmeier et al. (1997a))

Spectral type		O9.7Ib
Mass	$M_*$	$34 M_\odot$
Radius	$R_*$	$24 R_\odot$
Terminal speed	$v_\infty$	1850 km/s
Mass loss rate	$\dot{M}$	$3 \times 10^{-6} M_\odot \text{ yr}^{-1}$

onto the compact companion powers the high X-ray luminosity of  $\sim 10^{33} - 10^{39} \text{ erg s}^{-1}$ . HMXBs can be divided in subclasses depending on the spectral type of the donor star – supergiant (SG) or Be-star, and the type of variability – persistent or transient.

In this paper we consider SG HMXBs. The basic physics of neutron-star accretion in stellar winds was described in the seminal paper by Davidson & Ostriker (1973), who suggest that the Bondi-Hoyle-Lyttleton accretion powers the X-ray luminosity in HMXBs. Kallman & McCray (1982) presented theoretical models for the temperature and ionization structure of spherically symmetric, constant density, gaseous nebulae surrounding compact X-ray sources. Two-dimensional hydrodynamic simulations of the gas flow in the orbital plane of a massive X-ray binary system were presented by Blondin et al. (1990). The simulations revealed the presence of dense filaments of compressed gas formed in the non-steady accretion bow shock and wake of the compact object. The underlying assumption in all these models is an initially smooth donor stellar wind with the CAK density distribution. In a recent review, Edgar (2004) demonstrated that despite the simplifications made, Bondi-Hoyle-Lyttleton predictions for the accretion rate are quite accurate. Negueruela (2010) reviewed recent works on stellar wind accretion, and suggested that the real sources differ from the idealized situation of Bondi-Hoyle-Lyttleton accretion in three main ways: the winds of massive stars are highly structured; accretion to a compact object is an unstable process; and the magnetic field of the neutron star may affect the flow of material. In this paper we investigate the immediate consequences of stellar wind clumping for the accretion rate, wind ionization, and the absorption of X-rays in the unperturbed portion of the wind.

The observational evidence of clumped accretion flow in SG HMXBs is growing. Sako et al. (2003) reviewed spectroscopic results obtained by X-ray observatories for several wind-fed HMXBs. They concluded that the observed spectra can be explained only as originating in a clumped stellar wind where cool dense clumps are embedded in rarefied photoionized gas. van der Meer et al. (2005) studied the X-ray light curve and spectra of the HMXB 4U 1700-37. They showed that the feeding of the NS by a strongly clumped stellar wind is consistent with the observed stochastic variability.

in’t Zand (2005) proposed that the flaring behavior of supergiant fast X-ray transients (SFXT) can be explained by the accretion of wind blobs. This suggestion was corroborated by the studies of hard X-ray flares and quiescent emission of SFXT systems by Walter & Zurita Heras (2007), who estimated wind clump parameters and found them to be in agreement with the macroclumping paradigm of stellar winds. Negueruela et al. (2008) presented a common framework for wind accreting sources, in the context of clumpy wind models. They postulated that the different flaring behavior can be an immediate consequence of diverse orbital geometries.

Kreykenbohm et al. (2008) studied the temporal variability of Vela X-1. They interpreted flares and off states as being due to a

<sup>1</sup> Waldron & Cassinelli (2010) pointed out that the extreme UV radiation may be important for the mass-loss diagnostics based on resonant lines.

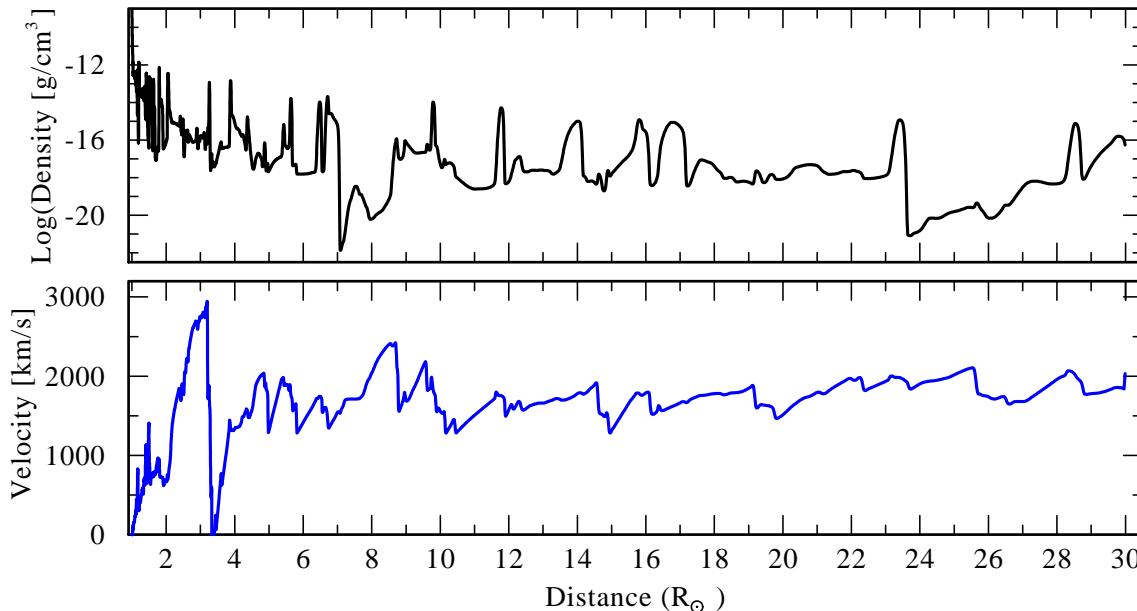


**Figure 1.** A snapshot of the density (upper panel) and the velocity (lower panel) structure of the stellar wind in a O9.5 supergiant star as predicted by time-dependent hydrodynamic simulations (Feldmeier et al. 1997a,b). The upper panel shows that the density fluctuations in the wind have many orders of magnitude, while the lower panel shows the strong wind velocity jumps.

strongly structured wind of the optical companion. They suggested that when the NS in Vela X-1 encounters a cavity with strongly reduced density, the X-ray flux drops, thus triggering the onset of the propellor effect, which inhibits further accretion (off states). From the analysis of the flaring behavior of Vela X-1 Fürst et al. (2010) concluded that a mixture of a clumpy wind, shocks, and turbulence can explain the flare brightness distribution. Sidoli et al. (2010) suggested that the X-ray variability of the HMXB IGR J08408–4503 may be explained by stellar wind clumping. Bozzo et al. (2011) observed a bright X-ray flare in the HMXB IGR J18410-0535. They concluded that the flare was produced by the accretion of massive clump onto the compact object hosted in this system.

Ducci et al. (2009) developed a phenomenological stellar wind model for OB supergiants to investigate the effects of accretion from a clumpy wind on the luminosity and variability properties of high-mass X-ray binaries. They concluded that the model can reproduce the observed light curves well. They also pointed out that the overall mass loss from the supergiant should be about a factor of 3–10 smaller than the values inferred from ultraviolet line studies that assume a homogeneous wind. This, as well as all other works on the phenomenology of clumped winds in HMXBs, account only for the presence of dense wind clumps and ignore the non-monotonic wind velocity.

In this paper we employ time-dependent hydrodynamic simulations of non-stationary stellar winds and use the predicted non-monotonic density and velocity fields to compute the accretion rate. We deliberately concentrate on the general consequences of stellar wind clumping for the HMXBs. Multi-D hydrodynamic models and the processes in the immediate vicinity of the compact object are beyond the scope of this paper. We consider here systems of intermediate and small X-ray luminosity, such that the donor stellar wind at large is not perturbed by the presence of the compact object and its X-ray emission.

The paper is organized as follows. In Sect. 2 we describe the hydrodynamic models used to obtain the time-dependent wind den-

sity and velocity. The Bondi-Hoyle-Lyttleton accretion formalism is applied in Sect. 3 to simulate the resulting time-dependent X-ray luminosity. The photoionization in the clumped wind is considered in Sect. 4. In Sect. 5 we apply our 2D model of a clumped stellar wind to predict the changes in absorption during the orbital motion of the NS. The discussion is presented in Sect. 6 and conclusions are drawn in Sect. 7.

## 2 HYDRODYNAMICAL SIMULATIONS

We employ the results of hydrodynamical simulations of the line driven stellar wind presented in Feldmeier et al. (1997a,b). These hydrodynamic simulations derive the dynamic and thermal structure of stellar winds from the basic underlying physical principle, namely the acceleration of stellar wind by the line scattering of stellar UV photons (CAK).

The simulations were performed using the smooth source function method (Owocki & Puls 1996). The line-driven instability (LDI) is handled by a careful integration of the line-optical depth with a resolution of three observer-frame frequency points per line Doppler width and by accounting for non-local couplings in the non-monotonic velocity law of the wind. The angle integration in the radiative flux is limited to one single ray which hits the star at  $\approx 0.7R_*$ . This accounts with sufficient accuracy for the finite-disk correction factor. The pure hydrodynamics part of the code is a standard van Leer solver. The seed perturbations for unstable growth, in the shape of turbulent variation of the velocity at a level of roughly one third of the sound speed, are introduced at the base of the wind. These perturbations have a coherence time in the friction term of 1.4 hr, which is not too far off the acoustic cutoff period of the star at which acoustic perturbations of the photosphere should accumulate. Further details can be found in Feldmeier (1995); Feldmeier et al. (1997a,b).

The hydrodynamic simulations were performed using stellar parameters of a typical late O-type supergiant star  $\zeta$  Orionis

(O9.7Ib) (see Table 1). A snapshot of a wind structure at some given moment of time is shown in Fig. 1. The variety of dynamical structures in the instability-induced, line-driven wind turbulence seems to be similarly intricate to that found in other turbulent flows in astrophysical MHD settings. There are indications of the presence of a quasi-continuous hierarchy of density and velocity structures in the wind. Dense shells are formed close to the star, in a first stage of unstable growth. These dense shells have rather small radial extent, and contain a large fraction of the wind mass. In the framework of these hydrodynamic models, the colloquial term “wind clumps” refers to these dense shells. The space between the shells is filled by tenuous and hot gas (Feldmeier et al. 1997a,b).

Further out in the wind, in a second stage of unstable growth, a somewhat different type of dense structures are formed: the small “clouds” that are “ablated” from the outer rim of the remaining mass reservoir at CAK densities, and are accelerated by the stellar radiation field through the emptied regions, eventually colliding with the next-outer shell. The X-ray emission from single early type star winds is explained by these cloud-shell collisions.

While the *average* velocity field follows the so-called  $\beta$ -law:

$$v(r) = v_\infty(1 - 1/r)^\beta, \quad (1)$$

where  $v_\infty$  is the wind terminal speed, there are strong velocity jumps with negative gradients across the shells. In Figure 2 we show the wind velocity at some specific radius in the wind as function of time. The figure illustrates, that relatively close to the star (we selected a radius  $2.5R_*$  from the stellar surface) the wind velocity changes by up to an order of magnitude on a time scale of hours.

### 3 ACCRETION OF A NON-STATIONARY STELLAR WIND

#### 3.1 Basics of Bondi-Hoyle accretion

The following is based on the treatment of Davidson & Ostriker (1973). They considered a neutron star of mass  $m_X$ , traveling at relative speed  $v_{\text{rel}}$  through a gas density  $\rho$ . If  $v_{\text{rel}}$  is supersonic, the gas flows in a manner described by Bondi & Hoyle (1944). The mass accretion rate is given by

$$S_{\text{accr}} = \pi \zeta r_{\text{accr}}^2 v_{\text{rel}} \rho(a, t) \quad (2)$$

where

$$r_{\text{accr}} = \frac{2Gm_X}{v_{\text{rel}}^2} \quad (3)$$

and the factor  $\zeta$  is intended to correct for radiation pressure and the finite cooling time of gas. In moderately luminous X-ray sources  $\zeta \lesssim 1$  (Davidson & Ostriker 1973). For our calculations we adopt  $\zeta = 1$ .

In non-stationary stellar winds, the wind density  $\rho(a, t)$  and the wind velocity  $v_w(a, t)$  depend on time (see Section 2). Combining equations (2) and (3) the accretion rate is

$$S_{\text{accr}} = 4\pi \zeta \frac{(Gm_X)^2}{v_{\text{rel}}^3} \rho(a, t). \quad (4)$$

The relative velocity

$$v_{\text{rel}}^2 = v_X^2(a) + v_w^2(a, t), \quad (5)$$

where  $v_w$  is the stellar wind velocity at the neutron star orbital separation  $a$ , and the orbital velocity of the neutron star is given by

$$v_X^2 \approx \frac{GM_*}{a}. \quad (6)$$

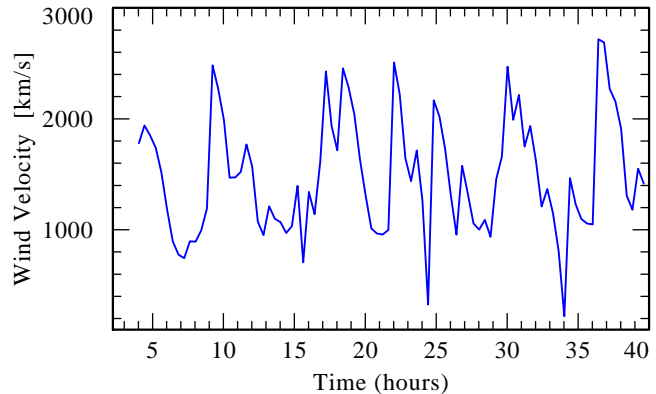


**Figure 2.** The model (see text) wind velocity as function of time at the radius  $a = 2.5 R_*$ . The amplitude of velocity variations may exceed order of magnitude in only few hours.

The X-ray luminosity of an accreting neutron star is then

$$L_X^d(a, t) = \eta S_{\text{accr}} c^2, \quad (7)$$

where  $c$  is the speed of light, and  $\eta$  is a constant depending on the exact physics of accretion and typically taken to be  $\eta \sim 0.1$ .

#### 3.2 Synthetic accretion light curves

The time dependent hydrodynamic simulations described in section 2 provide absolute values for the wind density and velocity as functions of radius and time for a star with parameters as shown in Table 1. We use these density and velocity to compute synthetic X-ray light curves according to Eqs. (4)–(7).

Adopting a mass of the compact object  $m_X = 1.4 M_\odot$  and an efficiency parameter  $\eta = 0.1$ , we generated simulated light curves for different values of the orbital separation  $a$ . The resulting predicted variations in X-ray luminosity  $L_X^d$  are shown in Fig. 3.

The synthetic light curves are highly variable, with X-ray luminosity changing by up to eight orders of magnitude! This strong variability is a consequence of the highly variable density and velocity in the stellar wind. Specifically we would like to emphasize that the shocks and corresponding jumps in the velocity with  $\delta v \sim 1000 \text{ km s}^{-1}$  are responsible for the predicted strong variability, since the accretion rate scales with  $\propto v^{-3}$ . Thus models which account only for the density fluctuations in the winds (e.g. Walter & Zurita Heras 2007; Ducci et al. 2009) may underestimate the resulting variability.

It is interesting to note, that the character of the light curves cannot be characterized as steady quiescent emission and some strong flares on top it. Reflecting the nature of non-stationary inhomogeneous stellar winds the accretion light curves are truly stochastic.

The X-ray observations of real celestial HMXBs are sensitive to the X-ray flux only about some threshold. In an arbitrary way we choose this threshold corresponding to the X-ray luminosity  $10^{34} \text{ erg s}^{-1}$ . Figure 4 shows the fraction of time the luminosity of model source is above this threshold. It demonstrates that the fraction of time the source is X-ray bright decreases sharply with increasing orbital separation. In HMXBs with larger orbital separation, the periods of highest accretion are significantly less frequent.

We calculate the average X-ray luminosity resulting from direct accretion,  $\bar{L}_X^d$ , the standard deviation  $\sigma_L$ , and the relative variability  $\sigma_L/\bar{L}_X^d$ . Our models show that there is no apparent depen-

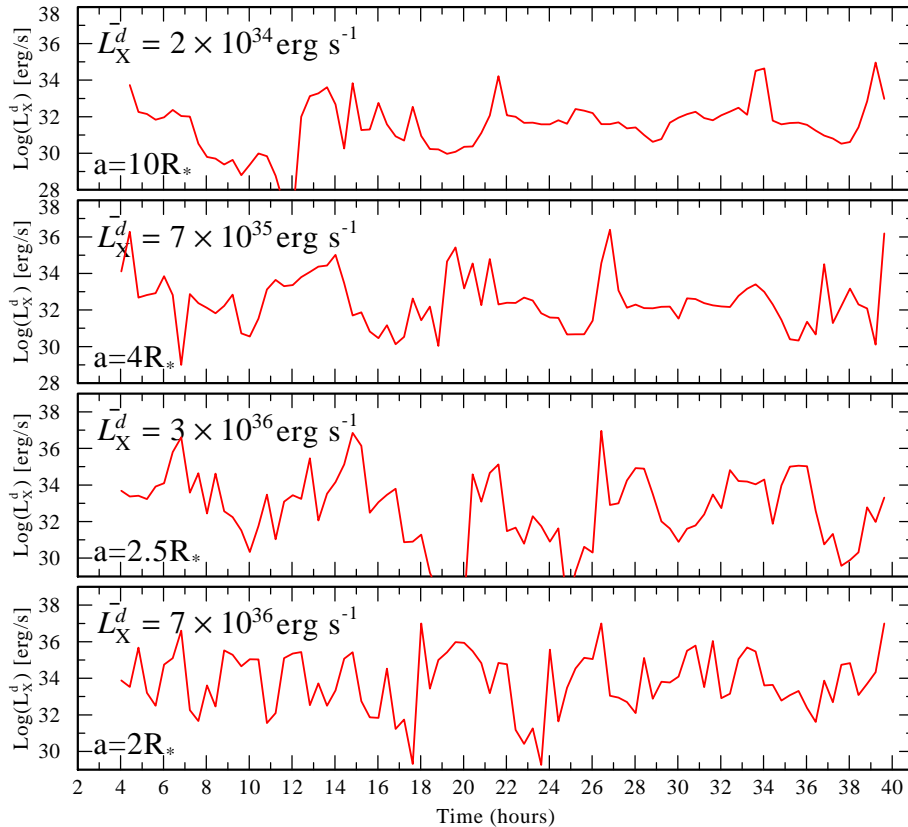


**Figure 3.** Synthetic X-ray light curves for Bondi-Hoyle accretion of a non-stationary stellar wind onto a neutron star with  $m_X = 1.4 M_\odot$ . The supergiant donor parameters are given in Table 1. From top to bottom panel, the orbital separation  $a$  is decreasing, as indicated in the lower left corner of each panel. The average X-ray luminosity is indicated in the upper left corner. The relative variability  $\sigma_L/\bar{L}_X^d = 4.8, 4.9, 4.9, 4.6$  from top to bottom panel.

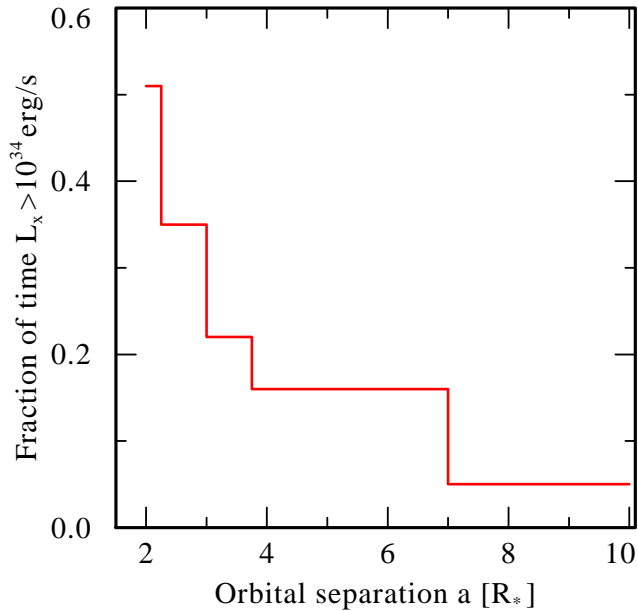


**Figure 4.** The fraction of time the synthetic accretion light curve is above the level  $10^{34} \text{ erg s}^{-1}$  in dependence on the orbital separation  $a$ .

dence of the relative variability on orbital separation within the parameter space we have chosen. This reflects the stochastic nature of stellar wind even relatively far from the stellar core.

#### 4 THE PHOTOIONIZATION PARAMETER IN THE CLUMPED WIND OF HMXBS

The total X-ray emission in HMXB results from direct accretion which we considered in the previous section as well as from the photoionized fraction of stellar wind. Due to the highly variable accretion rate, the ionizing source is highly variable (see Fig. 3). Moreover, the ambient stellar wind is highly inhomogeneous (see Fig. 1). In this section we investigate how the ionization parameter is changed in a clumped wind compared to a smooth medium – the latter is commonly adopted in the computations of spectra from photoionized plasma.

To study these effects we adopt a statistical approach, assuming a large number of clumps. The use of a statistical approach is convenient for at least two reasons. First, the non-stationary hydrodynamic simulations we presented in the previous section are 1D, and while they are well suited to compute the luminosity of the accreting point source, we need additional information to study spatially extended photoionized regions. Second, there are sophisticated photoionization codes, such as *xstar* (Kallman & Bautista 2001) that account realistically for atomic physics of photoionized gases. Using a statistical treatment of the clumped stellar wind, we attempt to find correction factors that would allow to adjust the input parameters for a photoionization code in order to reflect the wind inhomogeneity.

The fundamentals of interaction of X-ray sources with ambient stellar winds are developed in Tarter et al. (1969), Tarter & Salpeter (1969). Hatchett & McCray (1977) considered a model of a constant X-ray source immersed in a stellar wind from

its companion star. The stellar wind model was as predicted by the then recent CAK theory. These works consider a nebula gas of constant density  $N$  (or smooth density gradient) illuminated by a constant source of X-ray radiation. The ratio  $N_e/N$  is determined in each case from charge neutrality. Adopting Tarter et al. (1969) notations, neglecting absorption one may take for the mean primary photon intensity at frequency  $\nu$  at a distance  $r$  from the source

$$J(\nu)d\nu = \frac{L}{4\pi r^2} f(\nu, kT_X), \quad (8)$$

where function  $f(\nu, kT_X)$  describes the spectral shape of the X-ray radiation. The equation of ionization equilibrium for a homogeneous medium is

$$N(Z, z+1)N_e\alpha(T_e) = N(Z, z) \int J(\nu)\sigma(\nu)d\nu + N_e C(T_e), \quad (9)$$

where  $C$  is the collisional ionization rate and  $\sigma$  is the photoionization cross-section for the changing ionic charge  $z \rightarrow (z+1)$  of ion with nuclear charge  $Z$ ;  $\alpha$  is the total coefficient for recombination for  $(z+1) \rightarrow z$ .

As follows from Eq. (8) and Eq. (9) for an optically thin gas in local ionization and thermal balance, irradiated by a constant point source of X-rays of given spectral shape, only a single photoionization parameter must be specified in order to determine the ionization state and temperature of any local region of the gas:  $\xi \equiv L_X/Na^2$ , where  $N$  is the local atomic number density of the gas at the orbit of the X-ray source, and  $a$  is the distance from the center of the primary to the X-ray source.

In the medium where the density is inhomogeneous, Eq. (9) shall be rewritten as

$$\langle N(Z, z+1)N_e \rangle \alpha(T_e) = \langle N(Z, z) \rangle \int J(\nu)\sigma(\nu)d\nu + \langle N_e \rangle C(T_e), \quad (10)$$

where the averaging over some local volume is represented by the angular brackets. Considering Eq. (10) it is clear, that, in general, the ionization parameter  $\xi$  is not the same as in smooth density case. It is also clear, that in the medium with density fluctuations, the number of recombinations which is proportional to the density squared is enhanced compared to the number of ionizations which is proportional to the density. Therefore, in the clumped stellar wind, the photoionization parameter must be reduced compared to the smooth wind. Moreover, the size of the photoionized region will be reduced in a clumped wind compared to the smooth wind of the same mass-loss rate.

To describe the density fluctuations we follow Allen (1973) and define the wind inhomogeneity parameter

$$\mathcal{X} \equiv \frac{\langle N^2 \rangle}{\langle N \rangle^2}. \quad (11)$$

Then the root mean square (rms) local density is  $N_{\text{rms}} = \langle N \rangle \sqrt{\mathcal{X}}$ . The rms density describes in a statistical sense the magnitude of density variations.

Assuming that there are no dramatic changes in the ionization state over some local volume, we can write

$$\langle N(Z, z+1)N_e \rangle \approx \mathcal{X} \langle N(Z, z+1) \rangle \langle N_e \rangle, \quad (12)$$

In this case, the photoionization parameter for a clumped stellar wind is

$$\xi \equiv \frac{L_X}{\mathcal{X} \langle N \rangle a^2}, \quad (13)$$

i.e. it is reduced by factor  $\mathcal{X}$  compared to the smooth wind case.

The particle density averaged over some unite volume at distance  $r$ ,  $\langle N \rangle$  is defined by the continuity equation:

$$\langle N \rangle = \frac{\dot{M}}{4\pi\mu m_H v(r)r^2}, \quad (14)$$

where  $\mu$  is the mean molecular weight,  $m_H$  is the atomic mass unit, and  $v(r)$  is a stationary velocity law.

The simplest structure of a clumped wind is a two phase medium where all matter is clumped with dense clumps occupying only a small volume compared to the interclump medium filling the large volume. The interclump medium can be assumed void or filled with tenuous gas. In this case a volume filling factor  $f_V$  can be defined as the fraction of total volume  $V_{\text{tot}}$  that is filled by clumps:  $f_V \equiv V_{\text{cl}}/V_{\text{tot}}$ . If the interclump medium is void  $\mathcal{X} = f_V^{-1}$ . The clump density in such two phase medium is  $N_c = \mathcal{X} \langle N \rangle$ . If the interclump medium is not void, its particle number density can be approximated as:

$$N_{\text{ic}} \approx (1 - \mathcal{X} f_V) \langle N \rangle. \quad (15)$$

#### 4.1 On the clump optical depth

Equation (8) neglects the absorption of ionizing radiation. This condition may not be valid when clumps are optically thick for the ionizing radiation. In this section we investigate the restrictions on the clump parameters imposed by this condition. To do so we estimate the geometrical size a clump which has optical depth unity. Assume for simplicity that the interclump medium is void, so that  $f_V = \mathcal{X}^{-1}$ , the optical depth of an isotropic clump (i.e., with the same dimensions  $d_c$  in 3D) for the incident radiation at wavelength  $\lambda$  is

$$\tau_c(\lambda) = \rho_w \kappa_\lambda f_V^{-1} d_c R_*, \quad (16)$$

where  $R_*$  [cm] is the stellar radius,  $d_c$  is in the units of  $R_*$  and  $\kappa_\lambda$  [cm<sup>2</sup> g<sup>-1</sup>] is the mass absorption coefficient. The density of the cool wind ( $\rho_w$ ) can be defined from the continuity equation.

The clump dimension  $d_c$  can be derived from Eq. (16). Adopting  $\tau_c(\lambda) = 1$ :

$$d_c^{\tau=1} = \frac{f_V}{\tau_*(\lambda)} \cdot \left(1 - \frac{1}{r}\right)^\beta r^2. \quad (17)$$

where  $\tau_*$  is a parameter and a  $\beta$ -law for the velocity is assumed. If at some radius  $r$ , the clump size is larger than  $d_{\text{clump}}^{\tau=1}$ , such a clump is no longer optically thin for X-ray radiation at  $\lambda$ . The parameter  $\tau_*(\lambda)$  can be conveniently expressed as

$$\tau_*(\lambda) \approx 722 \frac{\dot{M}_{-6}}{v_\infty \mathcal{R}_*} \cdot \kappa_\lambda, \quad (18)$$

where  $\dot{M}_{-6}$  is the mass-loss rate in units  $10^{-6} M_\odot \text{ yr}^{-1}$ ,  $v_\infty$  is the terminal velocity in [km s<sup>-1</sup>], and  $\mathcal{R}_* = R_*/R_\odot$  (Oskinova et al. 2011).

The K-shell opacity of stellar wind is a strong function of wavelength, and can be taken as  $\kappa_\lambda \approx \kappa_0 \lambda^\gamma$ , with  $\gamma$  in the range 2–3, and  $\kappa_0$  a constant that depends on abundances (Baum et al. 1992; Ignace & Oskinova 1999). It follows from Eqs. (17) and (18) that the same clump can be optically thin at shorter wavelengths and optically thick at longer wavelengths.

Realistic values of the mass-absorption coefficient have to be computed using non-LTE model stellar atmosphere codes, such as, e.g., PoWR (Hamann & Gräfener 2004). The values of  $\kappa_\lambda$  for a sample of O-stars are given in e.g. Oskinova et al. (2006).

The SG HMXB are hard X-ray sources. The maximum of spectral energy distribution in Vela X-1 is at  $\approx 4 \text{ \AA}$  (e.g. Doroshenko et al. 2011). Using parameters of  $\zeta \text{ Ori}$  and assuming  $f_V = 0.1$ , at  $a = 2 R_*$ ,  $d_{\text{clump}}^{r=1}(\zeta \text{ Ori}) \approx 20 \kappa_\lambda^{-1}$ . I.e. at the distance  $2 R_*$  from the stellar core, only geometrically large clumps with diameter larger than  $\sim 0.5 R_*$  are optically thick for the ionizing radiation shortwards of  $10 \text{ \AA}$ .

Such a clump size appears rather large, therefore it is probably reasonable to assume that the wind clumps are optically thin for the ionizing radiation resulting from the accretion onto a NS <sup>2</sup>

## 4.2 Optically thin clumps

As shown above, the wind clumps are most probably thin for the hard X-ray emission resulting from the accretion on a compact object. In this case, the ‘‘microclumping’’ approximation can be used. If the mean primary photon intensity is described by Eq. (8), then in a two phase medium where  $\mathcal{X} = f_V^{-1}$ , the photoionization parameter can be written as

$$\xi = f_V \cdot \frac{L_X}{\langle N \rangle a^2}. \quad (19)$$

The meaning of Eq. (19) is that the ionization parameter in a clumped wind is reduced by a factor  $f_V$  when the average density at distance  $a$  is given by Eq. (14). Following Hatchett & McCray (1977) the nondimensional variable  $q \equiv \xi \langle N \rangle a^2 (L_X f_V)^{-1}$  describes the shape of the surfaces for which  $\xi = \text{constant}$ . In clumped stellar wind, the parameter  $q$  will be larger than in a smooth wind. Considering the case of constant wind velocity, it would mean that the radius of spherical photoionized region is smaller in clumped wind compared to the smooth wind. This is easy to understand recalling that the number of recombination is enhanced in clumped wind compared to smooth wind, while the number of ionizations remains the same.

Over the last decade there have been numerous studies to establish the degree of wind clumping in OB supergiants. Puls et al. (2006) analyzed a sample of 19 Galactic O-type supergiants/giants, covering spectral types O3 to O9.5 using multiwavelength observations in radio, IR, and optical. They used the conventional assumption of the interclump medium being void. It was found that the upper limit on the volume filling factor in the innermost region ( $r \lesssim 2 R_*$ ) of stars with  $H_\alpha$  in emission is about 0.25. It is likely that the winds of donor stars in HMXBs have similar properties. In this case, the ionization parameter should be reduced by a minimum factor of four to account for wind clumping.

Fullerton et al. (2006) analyzed 40 Galactic O-type stars by fitting stellar wind profiles to observations of the P V resonance doublet in the UV. The found that to reconcile mass-loss rates empirically inferred from the analysis of UV and radio/optical spectra, the volume filling factors must be  $f_V \lesssim 0.01$ . Similar conclusions were reached by Bouret et al. (2005) who found  $f_V \approx 0.04$  in an O-type supergiant and  $f_V \approx 0.02$  in an O-type dwarf. If these clumping factors were realistic, the ionization parameter  $\xi$  would have to be reduced by factors of 25 ... 100. Oskinova et al.

(2007) showed that correctly accounting for the wind porosity in the analysis of UV resonant lines eliminates the need for very small volume filling factors and that realistic values are rather  $f_V \sim 0.1$ . Sundqvist et al. (2011) also used the hydrodynamic models of Feldmeier et al. (1997a,b) and found that in these models the typical clumping factors are  $f_V^{-1} \sim 10$ . In this case, in the studies of the X-ray spectra from photoionized gas, the ionization parameter  $\xi$  should be reduced by a factor  $\lesssim 10$  in clumped wind models compared to the unclumped ones.

## 4.3 Clumps of arbitrary optical depth

While it is likely that the wind clumps are optically thin for the hard ionizing radiation, (see Section 4.1), for completeness in this section we consider a case of optically thick clumps. Accounting for the clumps of arbitrary optical depth in stellar atmosphere models is sometimes referred to as ‘‘macroclumping’’. If the optically thick structures,  $\tau_c \gtrsim 1$ , are present in the wind, the mean primary photon intensity of ionizing radiation  $J_\nu$  must be corrected for the absorption in the clumps

$$J_\nu = \frac{L_X}{4\pi r^2} \cdot f(kT) \cdot e^{-\bar{\tau}(r)}, \quad (20)$$

where  $f(kT)$  is a function of atomic parameters and temperature that describes the spectrum of the incident ionizing radiation, and  $\bar{\tau}$  is the effective optical depth of the clumped medium (Feldmeier et al. 2003).

At a distance  $R_X$  from the source of ionizing radiation the effective optical depth is

$$\bar{\tau} = \int_0^{R_X} n_C \sigma_C (1 - e^{-\tau_c}) dr_x, \quad (21)$$

where  $n_C(r) \propto v^{-1}(r)r^{-2}$  is the average number of clumps within a unit volume, and  $\sigma_C$  is the clump geometrical cross-section (Oskinova et al. 2008, 2011). Note that the stellar wind parameters  $\dot{M}$  and  $\kappa_\lambda$  appear in the expression for  $\bar{\tau}$  only indirectly via  $\tau_c$  given by Eq. (16). Besides stellar wind parameters, the effective optical depth also depends on the geometrical distribution of the clumps via  $n_C$  and  $\sigma_C$ . The clump cross-section is different for the different clump geometries, e.g. for the spherical clumps  $\sigma_C \propto d_C^2$ , while for the oblate clumps the cross-section depends on the clump orientation. In the limit of  $\tau_C \gg 1$ , the effective optical depth is fully determined by the geometrical distribution of clumps (Feldmeier et al. 2003; Oskinova et al. 2004).

Now we would like to address the question of ionization balance in the wind where the largest portion of the matter is in form of optically thick clumps. The X-ray emission from such medium will have two components: X-rays due to scattering of radiation within the clumps, and the X-rays from the photoionized interclump medium. The scattering of photons in such a medium was considered by Suleimanov et al. (2003). Here, we consider the ionization of the interclump medium and neglect the diffuse radiation. Using Eq. (15) for the particle number density in the interclump medium, the ionization parameter for the tenuous interclump gas becomes

$$\xi_{\text{ic}} = \frac{L_X}{\langle N \rangle a^2} \cdot \frac{e^{-\bar{\tau}}}{1 - \mathcal{X} f_V}. \quad (22)$$

When the bulk of stellar wind mass is in the form of a few dense optically thick clumps, the interclump medium can be very tenuous  $\mathcal{X} \rightarrow f_V^{-1}$ . In this case the effective optical depth can be very small (i.e. the wind is very porous). As follows from Eq. (22), in this case

<sup>2</sup> Note, that the intrinsic X-ray radiation in single SG OB stars is thermal and soft, with the maximum of the differential emission measure distribution at  $\approx 60 \text{ \AA}$  or even softer (e.g. Raassen et al. 2008). Even geometrically very small clumps with diameter  $10^{-3} \dots 10^{-5} R_*$  are optically thick at these wavelengths. Therefore, generally, in the inner wind regions of single SG OB stars the optically thin clump approximation for the intrinsic X-ray radiation is false.

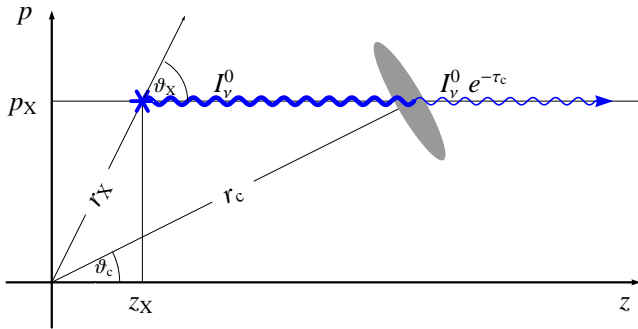


**Figure 5.** Sketch of the coordinate system for the fragmented wind model. X-ray radiation with intensity  $I_v^0$  is emitted at the location with coordinates  $(p_i, z_i)$ . The cool wind consists of clumps that are randomly distributed. For clarity, only one clump (shaded area) is shown in the sketch. The X-ray radiation propagating towards the observer at  $z \rightarrow \infty$  has to cross a clump. The optical depth for the ray in the  $z$  direction is  $\tau_c$ , reducing the line intensity  $I_v^0$  by a factor  $\exp(-\tau_c)$ .

the ionization parameter in the tenuous interclump gas can be very high, much higher than would be expected for the smooth wind of the same mass-loss rate.

We conclude that clumping strongly affects the ionization balance. A higher degree of ionization in the less dense interclump gas within the photoionized region can be expected. The size of the photoionized region will be much larger in case of optically thick clumps compared to a smooth wind.

## 5 ABSORPTION OF X-RAY RADIATION IN A CLUMPED STELLAR WIND

The X-ray photons emitted either in close vicinity to the NS, or farther out in the photoionized portion of the stellar wind, suffer the K-shell continuum absorption in the cool component of the stellar wind as they propagate towards the observer. As discussed in Sect. 4.1 the wind clumps are, most likely, optically thin for the radiation at the short wavelengths (shortward of  $\approx 8 \text{ \AA}$ ). On the other hand, the wind clumps or larger scale wind structures can be optically thick for the softer X-rays. These optically thick inhomogeneities can be traced observationally as changes in the absorbing column density on the time scale comparable to the orbital period. Such variability of absorbing column is indeed detected (e.g. Füst et al. 2011). If the stellar wind of donor star were smooth, the absorbing column would smoothly increase from the moment when the NS is at the periastron to when it is in the apastron.

In this section we investigate the K-shell continuous X-ray absorption in stellar wind. Our goal is to model the absorption of monochromatic X-ray flux emerging from the NS in dependence on orbital phase. We employ a 2D model of a stochastic stellar wind by Oskinova et al. (2004), where the model details are fully described. Here we only briefly introduce its basic features. The model assumes the structure and physical conditions in the wind according to the hydrodynamic simulations by Feldmeier et al. (1997a,b). The emission is decoupled from absorption, which allows for the formal solution of the radiative transfer equation. In order to take advantage of the rotational symmetry of our model around the  $z$  axis, cylindrical coordinates  $(p, z, \varphi)$  are used. Along each line of sight towards an X-ray emitting region located at spherical coordinates  $(r_i, \vartheta_i)$ , the emergent monochromatic X-ray intensity  $I^+(p, z, \varphi)$  is reduced by a factor

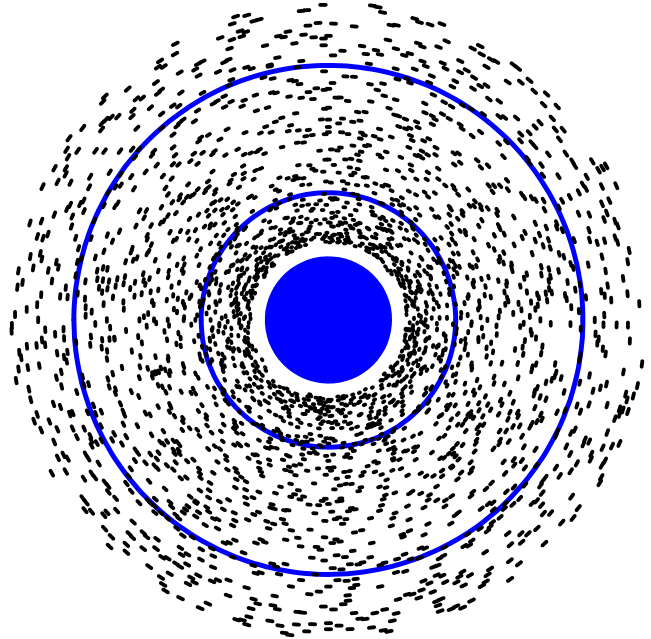


**Figure 6.** One random trial of our 2-D model where the clumps are randomly distributed in radius (uniformly between  $1.2$  and  $316 R_*$ ). On average there are 400 clumps along each radial direction (see text for details). Only the inner part of the wind between  $1R_*$  and  $5R_*$  is shown. The smooth wind is in-between  $1R_*$  and  $1.2R_*$ . The filled circle represents the stellar core; the outer circles are at  $2R_*$  and  $4R_*$  to scale. This random model was used to calculate optical depths shown in Fig., 8 and Fig., 7.

$\exp(-\tau(p, z, \varphi))$ :  $I^+(p, z, \varphi) = I^0(p, z, \varphi) \exp(-\tau(p, z, \varphi))$ . The optical depth  $\tau(p, z, \varphi)$  is given by the summation of optical depths of all clumps on the line of sight. The geometry of the model is shown in Fig. 5. Due to the lack of synchronization between different radial directions, the fragments probably have rather small lateral extent. Despite the expansion due to the internal pressure, the cool fragments are maintained to distances of hundreds of the stellar radius, before they gradually dissolve into a homogeneous outflow. Our 2-D stochastic wind model is designed to describe in a generic way the structures and physical conditions of the inhomogeneous stellar wind:

1. the flow is spherically symmetric in a statistical sense and propagates according to a  $\beta$  velocity law. The mass-flux and total radial optical depth in each radial direction is preserved.
2. all clumps cover the same solid angle as seen from the center of the star, and preserve this angle during their propagation.
3. we consider two different shapes of clumps, the spherically symmetric clumps (“balls”) and radially compressed clumps (“pancakes”).
4. to simulate stochastic X-ray emission we model X-rays as discrete random flashes of X-ray light along the NS orbit. There is no self-absorption by emitting material and no re-emission of X-rays which became absorbed by cool fragments.
5. we consider an edge on system, i.e. the observer is located in the orbital plane of the NS

We neglect the density fluctuations which are likely to result in the NS wake. The hydrodynamic simulations of wind structure that predict the existence of a wake were performed for smooth winds (Blondin et al. 1990). It is not obvious how accounting for wind clumping can affect the results of hydrodynamic simulations and



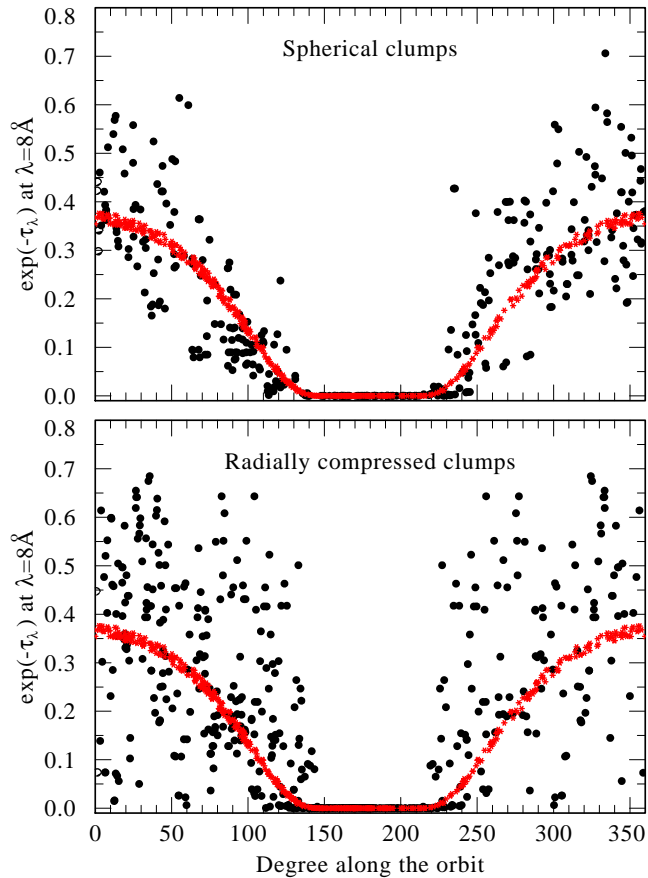


**Figure 7.** The variation of the factor  $\exp(-\tau_\lambda)$  in dependence on orbital phase for the X-ray radiation at  $8 \text{ \AA}$  ( $1.55 \text{ keV}$ ) emitted by a source located at  $\approx 2 R_*$ . The horizontal axis shows the orbital location of the X-ray source,  $\varphi_i$ . At  $0^\circ$  the source is in conjunction, while at  $180^\circ$  it is totally eclipsed. The red curve shows the changes of  $\exp(-\tau_\lambda)$  in a smooth wind. The parameters of the wind are given in Table 1. A velocity law with exponent  $\beta = 0.8$  is assumed. The stochastic wind model is calculated using the random trial shown in Fig. 6. *Upper panel:* the wind model where the clumps are assumed to be spherically symmetric (“balls”). *Lower panel:* the wind model where the clumps are assumed to be flattened in the radial direction (“pancakes”).

the shape and density in the wake. Moreover, the presence of the wake should introduce some regular pattern in the absorption of X-rays along the orbital motion of the NS, while our goal is to investigate the basic effects of stochastic winds on the absorption of X-rays.

We also neglect the changes in the ionization structure of the wind due to the X-ray photoionization close to the NS. As discussed in Section 4, the clumping is likely to reduce the size of photoionization zone. The optical depth of the clumps within the photoionized portion of the wind may be different from the rest of the wind, however this effect may be small on average due to the difference in the size of the general wind, and its photoionized portion.

Figure 6 shows a snapshot of the inner wind structure, between  $1 R_*$  and  $5 R_*$  (in the simulations clumping is maintained up to  $316 R_*$ ). We assume the lateral extend of clumps to be  $1^\circ$ . To study how the wind optical depth changes during the orbital motion of the NS, we assumed the donor stellar parameters as listed in Table 1. The clump number density obeys the continuity equation, therefore the clump density is higher in the innermost part of the wind and

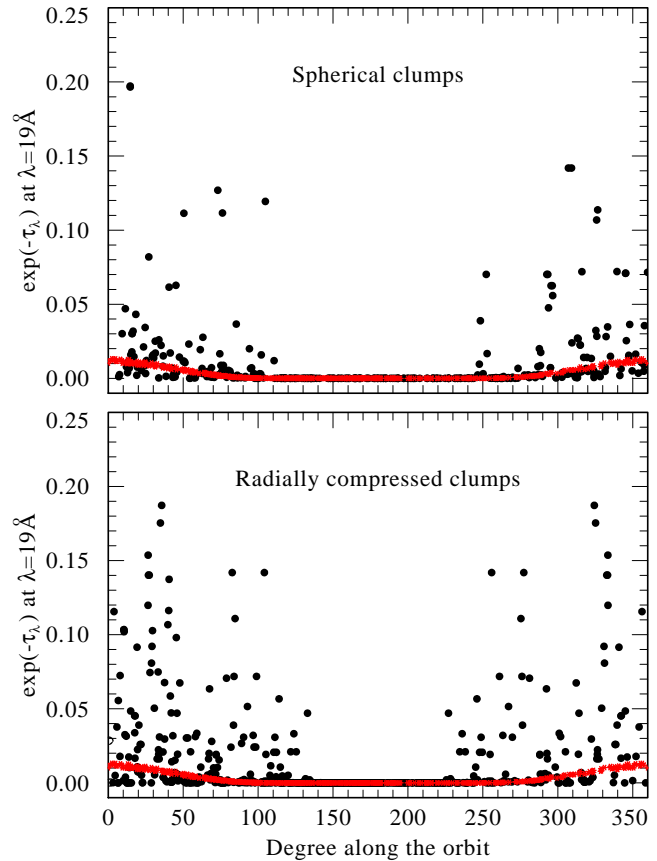


**Figure 8.** The same as in Fig. 7 but for the radiation emitted at  $19 \text{ \AA}$  ( $0.65 \text{ keV}$ ).

gradually decreases outwards. To find the optical depths towards the observer at different orbital location, we sum up the contributions from all the clumps along the line of sight.

The mass-flux in each direction is preserved in our model. To calculate the optical depth of each clump (in total there are 144 000 clumps in the wind model, part of which is shown in Fig. 6) we assume that a clump mass equals to the mass of the smooth wind confined between to random subsequent radii in the wind  $r_a$  and  $r_b$  (see Oskinova et al. (2004) for details). For a star with the parameters shown in Table 1 and solar abundances, the mass-absorption coefficient  $\kappa_\lambda$  is  $\approx 40 \text{ cm}^2 \text{ g}^{-1}$  at  $\lambda = 8 \text{ \AA}$  and  $\approx 170 \text{ cm}^2 \text{ g}^{-1}$  at  $\lambda = 19 \text{ \AA}$  (Oskinova et al. 2006).

Little is known about the geometrical shape of the clumps. The comparison with the observed X-ray emission line profiles in spectra of single O-stars indicate that the clumps can be flattened in radial direction (Oskinova et al. 2006). The shape of clumps plays an important role in the transfer of X-ray radiation through the wind: in case of flattened clumps the wind opacity becomes anisotropic, while it remains isotropic (the same as for the smooth wind opacity albeit smaller) in case of ball-like clumps (Oskinova et al. 2006).

Figures 7 and 8 show the transmission factor  $\exp(-\tau_\lambda)$  for radiation at  $8 \text{ \AA}$  and  $19 \text{ \AA}$  ( $1.55 \text{ keV}$  and  $0.65 \text{ keV}$ , respectively) calculated assuming different clump geometries and a smooth wind. The wind is more transparent for the radiation at shorter wavelengths. In case of flattened clumps the changes in optical depth are larger, because the clump optical depth depends on the clumps orientation.

The changes in the wind absorbing column at different orbital phases should result in changes in the X-ray spectra. Indeed, the

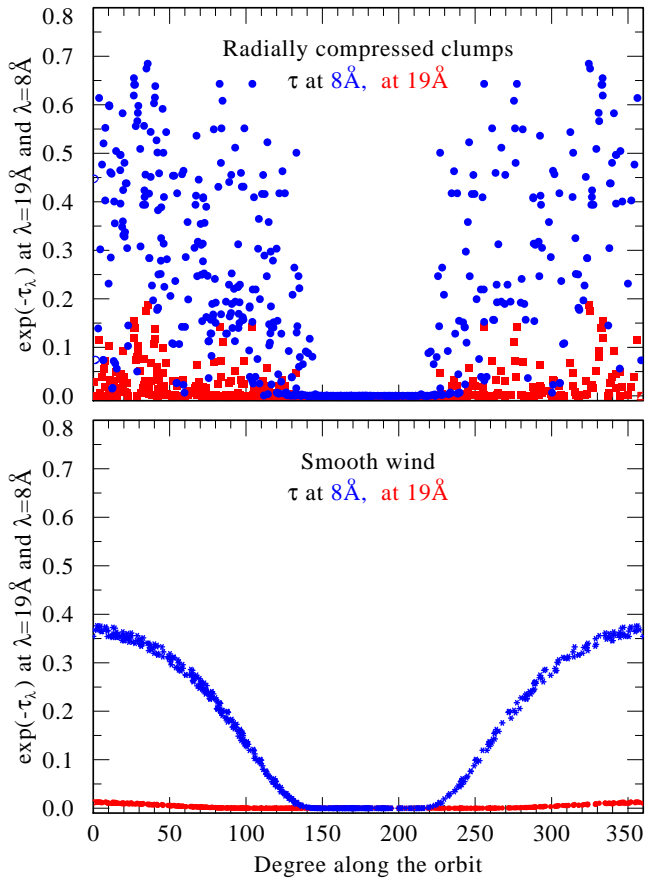


**Figure 9.** The same as in Fig. 8. *Upper panel:* comparing the  $\exp(-\tau_\lambda)$  factor at  $19 \text{ \AA}$  (red) and  $8 \text{ \AA}$  (blue) at different orbital phases for a model wind that consists of flattened clumps. *Lower panel:* the same as upper panel but for a smooth wind model.

strong variations of absorbing column density at different orbital phases are often deduced from the observed spectra (e.g. Fürst et al. 2010; Bozzo et al. 2011).

The K-shell absorption in stellar wind is strongly wavelength dependent, changing by a two orders of magnitude across the 0.1–12 keV X-ray band. This is reflected in smaller variations in the optical depths predicted for the  $8 \text{ \AA}$  radiation (where the wind opacity is smaller, Fig. 7) compared to the large optical depth variations at  $19 \text{ \AA}$  (where the wind opacity is larger, Fig. 8). The attenuation of X-ray radiation in a clumped wind has a weaker dependence on the wavelength than in a smooth wind (Oskinova et al. 2004). This prediction holds also for the HMXB. In Fig. 9 we compare the duration of the X-ray eclipse at two different wavelengths for clumped and smooth wind models. In a smooth wind, the eclipse at longer wavelength starts earlier, and lasts longer, while at shorter wavelength the eclipse is more narrow. On the other hand, in a clumped wind model, the difference between eclipse durations is less pronounced. Even in the phases close to the eclipse, optical depths may occasionally be as low as in the phases far from the eclipse.

## 6 DISCUSSION

It emerged from our analysis that the stellar wind clumping has drastic consequences for the phenomenology of SG HMXBs. The effect of wind structure on the accretion rate is profound. The hy-

drodynamic simulations predict wind structure consisting of strong velocity and density jumps. Since the Bondi-Hoyle-Lyttleton accretion rate depends on *both* velocity and density fluctuations, it strongly varies with time. Combining the Bondi-Hoyle model of accretion with hydrodynamic wind simulations we computed synthetic X-ray light curves for the different orbital separations (see Fig. 3).

Averaged over time model X-ray luminosity is in general agreement with observations. The moderate reduction of  $\dot{M}$  by factor 2 ... 3 compared to the unclumped wind models explains well the optical and the UV spectra of single stars, as well as average X-ray luminosity resulting from wind accretion in HMXBs.

The application of the Bondi-Hoyle-Lyttleton approximation for the accretion rate predicts very strong X-ray variability: the X-ray luminosity changes by many orders of magnitude on the time scale of hours as a direct consequence of the strong density and velocity jumps in the accretion flow. The effect of the non-stationary wind velocity on the accretion rate was overlooked previously. Neglecting this effect may lead to erroneous estimates of clump mass and size from the total flux and duration of the X-ray flare. We emphasize that the strong velocity jumps in the stellar winds lead to strong variability of accretion X-ray luminosity.

The detailed comparison of model light-curves and the observations will be a focus of our forthcoming study. However, it appears safe to conclude, that the synthetic light-curves do not agree well with the observations over-predicting the amplitude of variability. Given our simple approximation for the accretion this is not surprising. The detailed hydrodynamic studies that wind accretion is a highly complex process. E.g. when there is a density and velocity gradient in the flow, a transfer of angular momentum can become possible. The hydrodynamics of Bondi-Hoyle-Lyttleton accretion in a medium with continuous density and velocity gradients was considered by Ruffert (1997, 1999) and Fogliizzo et al. (2005). To our knowledge, up to now there were no studies of accretions from a medium with strong velocity and density jumps. We speculate that the detailed physics of the accretion flows regulates the temporal behavior of accretion and is pivotal in damping the strong variations due to the structured nature of stellar winds.

Another process that can reduce the variability is the destruction of clumps in the vicinity of the NS. As an interesting example of clump destruction, Pittard (2007) performed a hydrodynamical simulation of wind-wind collision in massive non-degenerate binary star. The simulations revealed that the clumps are rapidly destroyed after passing through the confining shocks of the wind-wind collision region (assuming adiabatic flow in the wind collision region). Despite large density and temperature fluctuations in the postshock gas, the overall effect of the interaction is to smooth the existing structure in the winds. One may speculate that in conceptually similar fashion, the wind clumps and the wind velocity gradients are “smoothed out” in the strong shock of the accretion wake in HMXBs.

Fürst et al. (2010) found that the accreted clump masses derived from the INTEGRAL data on Vela X-1 are on the order of  $5 \times 10^{19} - 10^{21} \text{ g}$ . Bozzo et al. (2011) estimate a mass and a radius of a clump responsible for a flare in a SFXT as  $\sim 10^{22} \text{ g}$  and  $\sim 10^{12} \text{ cm}$  correspondingly. These are important independent estimates of a clump mass that can be compared with what we know about clumps in single stars. Lépine & Moffat (1999) found stochastic line profile variations in the form of narrow ( $\approx 100 \text{ km s}^{-1}$ ) emission sub-peaks on top of emission lines in Wolf-Rayet star winds. They explained their data by  $10^3 \lesssim N_C \lesssim 10^4$  “blobs” being present at any time in the line emission region. In Oskinova et al. (2006) we reproduced

the Chandra observations of O-star X-ray line profiles by adopting a dynamic picture from Feldmeier et al. (1997a,b) hydrodynamic simulations – in each radial direction a clump is ejected once per dynamic time scale  $t_{\text{fl}} = R_*/v_\infty$ , which corresponds to a radial separation of one stellar radius when  $v_\infty$  is reached. Assuming that the wind consists of  $N_C$  clumps, an average clump mass  $M_C$  is

$$M_C \approx 4.4 \times 10^{25} \frac{\dot{M}_{-6} R_*}{v_\infty N_C} \text{ [g]} \quad (23)$$

Adopting a mass-loss rate  $\dot{M}_{-6} = 1 [10^{-6} M_\odot \text{ yr}^{-1}]$ ,  $v_\infty = 2000 \text{ [km s}^{-1}]$ , and  $R_* = 10 R_\odot$  with  $N_C \sim 10^4 \dots 10^5$  clumps in the wind, the average mass of a clump is  $M_C \sim 10^{18} \dots 10^{19} \text{ g}$ . These numbers compare very well with those independently found by Fürst et al. (2010) from the analysis of the INTEGRAL light-curves.

In this study we briefly addressed the absorption of X-rays in clumped stellar wind. We found that the wind optical depth strongly varies in dependence on orbital phase. We neglect the photoionization wake. Partly, this can be justified, because not much is known about the driving of X-ray photoionized clumped winds. Classically, the works that predict the decrease of driving force in the X-ray photoionized part of the outflow consider a smooth wind (MacGregor & Vitello 1982; Stevens 1988; Feldmeier et al. 1996). In clumped wind the ionization balance may be altered, e.g. the low ionization stage that can drive stellar wind may be still present within the clumps. Our investigation of changing optical depth in the wind around the compact object orbit demonstrates the potential of high-quality X-ray observations of SG HMXBs to provide much needed detailed information about the parameters of wind clumping. E.g. the orientation of the clumps, their distribution, can be studied from the changing absorbing column in stellar wind, especially during the X-ray eclipse.

The important result of our study, is that the ionization parameter is affected by the wind clumping. This follows from the basic fact that in the medium with density fluctuations, the recombination process ( $\rho^2$ -dependent) have priority over the photoionization process ( $\rho$ -dependent). The clumping of stellar wind is an established fact, and the ionization parameter must be corrected for the clumping in the analyses of spectra of photoionized gas in HMXBs. The ionization structure, the temperature, and the size of photoionized region is different in the clumped stellar wind compared to a smooth wind with the same mass-loss rate.

## 7 CONCLUSIONS

1. The results of time dependent hydrodynamical models of stellar winds predict a highly variable rate of wind accretion onto a compact object. The variability is largely due to the strong variations in the wind velocity (shocks). The highly non-uniform wind density also contributes to the variability of accretion rate.

2. Combining the Bondi-Hoyle model of accretion with hydrodynamic wind simulations predicts variability on stronger levels than commonly observed.

3. The X-ray light curves synthesized under the assumption of direct accretion predict strong variability of few orders of magnitude. The relative variability  $\sigma_L/\bar{L}_x^d$  has no strong dependence on the binary orbital separation.

4. The photoionization parameter depends on the properties of wind clumping. In optically thin case, the photoionization parameter has

to be reduced by the factor  $\mathcal{X}$  compared to the smooth wind model, where  $\mathcal{X}$  is the wind inhomogeneity parameter.

5. The absorption of X-rays in a clumped stellar wind strongly varies with the orbital phase. The degree of variability depends on the shape of the wind clumps, and is stronger for radially compressed clumps.

6. In a clumped wind, the wavelength dependence of the duration of the soft X-ray eclipse is smaller compared to the smooth wind models.

Overall, we conclude that the clumped non-stationary nature of the wind from the donor star strongly affects the X-ray light curve and leads to strong variability.

## ACKNOWLEDGMENTS

This research has made use of NASA's Astrophysics Data System Service and the SIMBAD database, operated at CDS, Strasbourg, France. The paper benefited from the useful remarks and suggestions of the referee, J. Sundquist, for which we are thankful. Funding for this research has been provided by DLR grant 50 OR 1101 (LMO). The research presented here benefited from many useful discussions with J. Wilms, I. Kreykenbohm, M. Hanke. The hospitality of Karl Remeis-Sternwarte, Universität Erlangen-Nürnberg, is greatly appreciated. LMO is very grateful for the hospitality and the simulating research environment of the ESA/ESAC Faculty.

## REFERENCES

- Allen C. W., 1973, *Astrophysical quantities*, Allen, C. W., ed.  
 Baum E., Hamann W., Koesterke L., Wessolowski U., 1992, *A&A*, 266, 402  
 Blondin J. M., Kallman T. R., Fryxell B. A., Taam R. E., 1990, *ApJ*, 356, 591  
 Bondi H., Hoyle F., 1944, *MNRAS*, 104, 273  
 Bouret J., Lanz T., Hillier D. J., 2005, *A&A*, 438, 301  
 Bozzo E., Giunta A., Cusumano G., Ferrigno C., Walter R., Campana S., Falanga M., Israel G., Stella L., 2011, *A&A*, 531, A130+  
 Castor J. I., Abbott D. C., Klein R. I., 1975, *ApJ*, 195, 157  
 Davidson K., Ostriker J. P., 1973, *ApJ*, 179, 585  
 Dessart L., Owocki S. P., 2005, *A&A*, 437, 657  
 Doroshenko V., Santangelo A., Suleimanov V., 2011, *A&A*, 529, A52+  
 Ducci L., Sidoli L., Mereghetti S., Paizis A., Romano P., 2009, *MNRAS*, 398, 2152  
 Edgar R., 2004, *New A Rev.*, 48, 843  
 Eversberg T., Lepine S., Moffat A. F. J., 1998, *ApJ*, 494, 799  
 Feldmeier A., 1995, *A&A*, 299, 523  
 Feldmeier A., Anzer U., Boerner G., Nagase F., 1996, *A&A*, 311, 793  
 Feldmeier A., Kudritzki R., Palsa R., Pauldrach A. W. A., Puls J., 1997a, *A&A*, 320, 899  
 Feldmeier A., Oskinova L., Hamann W., 2003, *A&A*, 403, 217  
 Feldmeier A., Puls J., Pauldrach A. W. A., 1997b, *A&A*, 322, 878  
 Foglizzo T., Galletti P., Ruffert M., 2005, *A&A*, 435, 397  
 Fullerton A. W., Massa D. L., Prinja R. K., 2006, *ApJ*, 637, 1025  
 Fürst F., Kreykenbohm I., Pottschmidt K., Wilms J., Hanke M., Rothschild R. E., Kretschmar P., Schulz N. S., Huenemoerder D. P., Klochov D., Staubert R., 2010, *A&A*, 519, A37+

- Fürst F., Suchy S., Kreykenbohm I., Barragán L., Wilms J., Pottschmidt K., Caballero I., Kretschmar P., Ferrigno C., Rothschild R. E., 2011, *A&A*, 535, A9
- Hamann W., Gräfener G., 2004, *A&A*, 427, 697
- Hamann W., Koesterke L., 1998, *A&A*, 335, 1003
- Hatchett S., McCray R., 1977, *ApJ*, 211, 552
- Hillier D. J., 1991, *A&A*, 247, 455
- Iben Jr. I., Tutukov A. V., Yungelson L. R., 1995, *ApJS*, 100, 217
- Ignace R., Oskinova L. M., 1999, *A&A*, 348, L45
- in't Zand J. J. M., 2005, *A&A*, 441, L1
- Kallman T., Bautista M., 2001, *ApJS*, 133, 221
- Kallman T. R., McCray R., 1982, *ApJS*, 50, 263
- Kreykenbohm I., Wilms J., Kretschmar P., Torrejón J. M., Pottschmidt K., Hanke M., Santangelo A., Ferrigno C., Staubert R., 2008, *A&A*, 492, 511
- Lépine S., Moffat A. F. J., 1999, *ApJ*, 514, 909
- , 2008, *AJ*, 136, 548
- Lucy L. B., 1982, *ApJ*, 255, 278
- Lucy L. B., Solomon P. M., 1970, *ApJ*, 159, 879
- Lucy L. B., White R. L., 1980, *ApJ*, 241, 300
- MacGregor K. B., Vitello P. A. J., 1982, *ApJ*, 259, 267
- Markova N., Puls J., Scuderi S., Markov H., 2005, *A&A*, 440, 1133
- Negueruela I., 2010, in *Astronomical Society of the Pacific Conference Series*, Vol. 422, *High Energy Phenomena in Massive Stars*, J. Martí, P. L. Luque-Escamilla, & J. A. Combi, ed., pp. 57–+
- Negueruela I., Torrejón J. M., Reig P., Ribó M., Smith D. M., 2008, in *American Institute of Physics Conference Series*, Vol. 1010, *A Population Explosion: The Nature & Evolution of X-ray Binaries in Diverse Environments*, R. M. Bandyopadhyay, S. Wachter, D. Gelino, & C. R. Gelino, ed., pp. 252–256
- Oskinova L., Hamann W., Ignace R., Feldmeier A., 2011, *Bulletin de la Societe Royale des Sciences de Liege*, 80, 54
- Oskinova L. M., Feldmeier A., Hamann W., 2004, *A&A*, 422, 675
- , 2006, *MNRAS*, 372, 313
- Oskinova L. M., Hamann W., Feldmeier A., 2007, *A&A*, 476, 1331
- Oskinova L. M., Hamann W.-R., Feldmeier A., 2008, in *Clumping in Hot-Star Winds*, W.-R. Hamann, A. Feldmeier, & L. M. Oskinova, ed., p. 203
- Owocki S. P., Castor J. I., Rybicki G. B., 1988, *ApJ*, 335, 914
- Owocki S. P., Puls J., 1996, *ApJ*, 462, 894
- Pittard J. M., 2007, *ApJ*, 660, L141
- Prinja R. K., Massa D. L., 2010, *A&A*, 521, L55+
- Puls J., Markova N., Scuderi S., Stanghellini C., Taranova O. G., Burnley A. W., Howarth I. D., 2006, *A&A*, 454, 625
- Raassen A. J. J., van der Hucht K. A., Miller N. A., Cassinelli J. P., 2008, *A&A*, 478, 513
- Ruffert M., 1997, *A&A*, 317, 793
- , 1999, *A&A*, 346, 861
- Runacres M. C., Owocki S. P., 2002, *A&A*, 381, 1015
- Sako M., Kahn S. M., Paerels F., Liedahl D. A., Watanabe S., Nagase F., Takahashi T., 2003, *ArXiv Astrophysics e-prints*
- Shklovsky I. S., 1967, *ApJ*, 148, L1+
- Sidoli L., Esposito P., Ducci L., 2010, *MNRAS*, 409, 611
- Stevens I. R., 1988, *MNRAS*, 232, 199
- Stewart G. C., Fabian A. C., 1981, *MNRAS*, 197, 713
- Suleimanov V., Meyer F., Meyer-Hofmeister E., 2003, *A&A*, 401, 1009
- Sundqvist J. O., Puls J., Feldmeier A., 2010, *A&A*, 510, A11+
- Sundqvist J. O., Puls J., Feldmeier A., Owocki S. P., 2011, *A&A*, 528, A64+
- Tarter C. B., Salpeter E. E., 1969, *ApJ*, 156, 953
- Tarter C. B., Tucker W. H., Salpeter E. E., 1969, *ApJ*, 156, 943
- van der Meer A., Kaper L., di Salvo T., Méndez M., van der Klis M., Barr P., Trams N. R., 2005, *A&A*, 432, 999
- Waldron W. L., Cassinelli J. P., 2001, *ApJ*, 548, L45
- , 2010, *ApJ*, 711, L30
- Walter R., Zurita Heras J., 2007, *A&A*, 476, 335